Monolayers of Symmetric Triblock Copolymers at the Air−Water Interface. 1. Equilibrium Properties

Mercedes G. Muñoz,[†] Francisco Monroy,*[,‡] Francisco Ortega,[†] Ramón G. Rubio,[†] and Dominique Langevin[‡]

Departamento de Química Física I, Facultad de Ciencias Químicas, Universidad Complutense, E28040 Madrid, Spain, and Laboratoire de Physique des Solides, LPS CNRS, Bâtiment 510, Université Paris-Sud, F91405 Orsay, France

Received February 10, 1999. In Final Form: October 1, 1999

Surface pressure isotherms and ellipsometric measurements of monolayers of two triblock symmetric copolymers, poly(ethylene oxide)−poly(propylene oxide)−poly(ethylene oxide) (PEO−PPO−PEO), at the air−water interface have been carried out. These copolymers are water-soluble, and the difference in hydrophobicity between the blocks is small. This represents a different scenario for brush formation than for most of the hydrophobic−hydrophilic block copolymers reported so far. The surface pressure curves show two different phase transitions. The ellipsometric measurements indicate a thickness transition when the monolayer saturates, which supports the hypothesis for brush formation. The experimental data have been analyzed in terms of the scaling theory of adsorption of polymer brushes. Despite the possibility of diffusion from the interface, the PPO block acts as an efficient anchoring element in the formation of an adsorbed brush, once the adsorption sites at the interface are fully occupied. This is analogous to what has been reported for diblock copolymers with a much larger difference in the hydrophobicity of the blocks.

1. Introduction

Since the pioneering works of Langmuir,[1] monomolecular layers at fluid interfaces have been the subject of many experimental and theoretical studies. The earliest studies on small amphiphilic insoluble monolayers revealed the existence of phase transitions in these bidimensional systems, usually known as Langmuir monolayers.[1,2] Recent experimental techniques, such as Brewster angle and fluorescence microscopy and small-angle X-ray or neutron reflectivity, have evidenced a rich phase behavior in this type of monolayers. In particular, gas and liquid expanded phases have been observed in the low surface pressure and low density regions of the phase diagram, while a wide variety of highly structured condensed phases have been found at higher pressures.[3] On the other hand, since diffusive exchange with the bulk phase is possible, high-density condensed states are not generally observed in adsorbed monolayers of soluble amphiphiles, also called Gibbs monolayers. The condensed states are unstable to compression, forcing the surfactant in excess to dissolve in the adjacent bulk solution. This is well illustrated by the fact that the collapse area per molecule of insoluble fatty alcohols (C_n−OH, $n > 12$) at the air−water interface, $A_\infty \approx 19$ Å^2/molecule, is smaller than the saturation area of the adsorbed monolayers of the smaller soluble homologous ($n < 10$), $A_\infty \approx 29$ Å^2/molecule.[4] Only a few studies describe the coexistence of two condensed phases in adsorbed or Gibbs monolayers of small surfactants.[5,6] In the earlier ones, the observed structures are believed to be caused by insoluble or sparingly soluble impurities. Only very recently, Melzer et al.[7] have clearly pointed out a first-order transition in adsorbed monolayers of a soluble *n*-alkyl amide, from a typical liquid expanded phase to a highly ordered condensed phase. The combined use of Brewster angle microscopy and grazing X-ray diffraction from a synchrotron source has allowed the comparison of this phase with that of an insoluble homologous surfactant at the same surface pressure Π. The morphological and structural equivalence between the two crystalline phases has been inferred from this study, which is the first clear evidence for phase coexistence in Gibbs monolayers.

In general, quasi-two-dimensional layers of long-polymer chains at the air−water interface do not show the complex phase behavior of small surfactants. This is due to the fact that crystalline order is not usually found unless strong stereoregularity constraints are fulfilled. However, it is also well accepted that adsorbed polymer layers can be obtained in several different configurations depending on polymer−interface and polymer−polymer interactions.[8] Consequently, one may expect phase transitions to occur between different states in films made of soluble hydrophilic polymers. In particular, weak surface adsorption, driven by polymer−interface hydrophobic forces, is expected to occur at low bulk concentrations. However, a *brush* phase made of chains grafted to the interface is expected at higher concentrations where the scarcity of adsorption sites in the interface favors a tridimensional arrangement stabilized by chain−chain and solvent−chain interactions.[9] This scenario is supported by many theoretical[9−12] and experimental studies. These focus mainly on the characteristic of the study of

* To whom correspondence should be addressed. E-mail: monroy@eucmos.sim.ucm.es.

[†] Universidad Complutense.

[‡] Université Paris-Sud.

(1) Gaines, G. L. *Insoluble Monolayers at Liquid−Gas Interfaces*; Interscience: New York, 1966.

(2) Harkins, W.; Boyd, E. *J. Chem. Phys.* **1941**, *45*, 20.

(3) Knobler, C. M. *Adv. Chem. Phys.* **1990**, *77*, 397.

(4) Lucassen-Reynders, E. H. *Prog. Surf. Membr. Sci.* **1976**, *10*, 253.

(5) Berge, B.; Faucheux, L.; Schwab, K.; Libchaber, L. *Nature* **1991**, *350*, 322.

(6) Rivière, S.; Hénon, S.; Meunier, J. *Phys. Rev. E* **1994**, *49*, 1375.

(7) Melzer, V.; Volhardt, D.; Weidemann, G.; Brezesinski, G.; Wagne, R.; Möhwald, H. *Phys. Rev. E* **1998**, *57*, 901.

(8) Fleer, G. J.; Cohen-Stuart, M. A.; Cosgrove, T.; Vincent, B. *Polymer at Interfaces*; Chapmann and Hall: London, 1993.

(9) Halperin, A. *Soft Order in Physical Systems*; Plenum: New York, 1994.

(10) Milner, S. T. *Science* **1991**, *251*, 905.

(11) Halperin, A.; Tirrell, M.; Lodge, T. P. *Adv. Polym. Sci.* **1991**, *100*, 31.

10.1021/la990142a CCC: $18.00
Published on Web 00/00/0000 PAGE EST: 10.9

the variation of the polymer concentration profile in the interface.[13−15]

In many of these works, the high hydrophobicity of one of the blocks made the copolymers effectively insoluble in the subphase. Under these conditions, both polymer adsorption with grafting at the air−water interface and block-associating mediated 2D micellization may occur. Indeed, the two phenomena would take place at constant surface pressure. However, in a solution of such polymers, with small blocks, it seems more plausible that most of the hydrophilic segments will remain dissolved in the bulk while the hydrophobic ones become anchored to the surface. On the other side, 2D micellization may be expected if the hydrophobic segments are long enough.[16] The grafting scenario has been recently studied, both theoretically and experimentally, by Barentin et al.,[17,18] for polymers with a strong difference of the hydrophilic−hydrophobic character of the blocks.

In the present work, we have studied the behavior of two symmetric triblock poly(ethylene oxide) (PEO)−poly(propylene oxide) (PPO)−poly(ethylene oxide) (PEO) copolymers at the air−water interface. A significant difference with previous studies is that the copolymers are fully soluble in water at room temperature, although they present a lower consolute critical point at higher temperatures. Despite the solubility of these polymers, the central more hydrophobic PPO blocks may act as anchoring elements at the air−water interface, while the more hydrophilic lateral PEO blocks dissolve in the bulk solution at sufficiently high surface concentration. In such a situation a polymer brush might be formed at the air−water interface. Further increasing the bulk concentration will cause the saturation of the brush, and no more polymer will be adsorbed at the interface; at this moment Π might remain constant, even if there is no micelle formation in the bulk. The CMC at 298 K is about 10 mM. We believe that 2D micellization seems a less plausible scenario for these fully water-soluble triblock polymers than for the extensively studied hydrophobic−hydrophilic diblock copolymers (PS−PEO, PDMS−PEO, etc., ...), where PS stands for poly(styrene) and PDMS for poly(dimethylsiloxane). Such systems are particularly interesting to look for a brush-forming system by weak preferential adsorption at the air−water interface.

The rest of this paper is organized as follows: A brief background on polymer brushes is presented in section 2. Section 3 summarizes the experimental details. The experimental results are presented in section 4 and discussed in section 5. Finally, the main conclusions are given in section 6. In the following paper in this issue (part 2), dynamic surface tension $\gamma(t)$ measurements will be combined with time-resolved ellipsometry to discuss the adsorption kinetics of these polymers in the full-adsorption planar monolayer regime and in the brush regime.

2. Polymer Brushes

Let us consider polymer chains attached to a solid or a liquid surface in the presence of other polymer molecules in solution. When the interchain space at the interface is less than the Flory radius in the solution, the chains stretch away from the surface and into the solvent, while remaining attached to the interface by an anchoring end; such a structure is called a polymer brush.[10,19,20]

These ideas, originally developed for homopolymers with an anchoring terminal group, can be extended to copolymers. In fact, both self-consistent field calculations[21,22] and scaling theories[23] point out the strong dependence of the internal structure of the adsorbed layer on the relative fraction of adsorbing and nonadsorbing blocks. In this scenario, block copolymers with hydrophobic and hydrophilic blocks are good candidates for grafting at air−water or oil−water interfaces.[24,25] Recently, from $\Pi-A$ measurements Barentin et al.[17,18] have found evidences for grafting in monolayers of *n*-alkyl end-capped PEO chains ($C_n-PEO-C_n$) at the air−water interface, favored by the insoluble character of the alkyl ends. In fact, an additional increase of the surface pressure with respect to the pure PEO isotherm was observed at a concentration higher than the accepted value for dissolution in the bulk of the pure POE chains, Γ_1 ($=1/A_1$, with $A_1 \approx 13$ Å^2/monomer).[26,27] Similar observations were made later by Fauré et al.[28] in monolayers of diblock PEO−PS copolymers, where the hydrophobic PS block acts as the anchoring element at the air−water interface. The equilibrium behavior and the adsorption kinetics observed in the monolayers of such hydrophobic−hydrophilic polymers are in excellent agreement with the theoretical predictions for polymer brushes anchored to an attractive wall.[15,29,30]

In general, for the polymers considered in this study, three regimes are proposed.[17,18,29,32] First, at sufficiently low surface concentration ($\Gamma < \Gamma_1$), all the monomers are adsorbed at the interface and form a dilute, $\Gamma < \Gamma^*$, or semidilute, $\Gamma^* \le \Gamma < \Gamma^{**}$ ($\le \Gamma_1$), solution in two dimensions. At higher concentration, $\Gamma > \Gamma_1$, the surface excess of the highly soluble blocks is stored in the bulk region near the interface. Finally the monolayer forms a thick brush at $\Gamma = \Gamma_2$, where the polymer chains overlap and stretch in the direction normal to the surface, avoiding each other.

3. Materials and Experimental Techniques

3.a. Chemicals. Two different symmetrical $(PEO)_A-(PPO)_B-(PEO)_A$ triblock copolymers (Pluronic) of different molecular weights and relative chain lengths (A/B) have been used in this study. Both polymers, hereinafter *Pluronic I* (Synperionic F68 from Fluka, Germany) and *Pluronic II* (from PolySciences, Germany), were used as received without further purification. They are fully soluble in water, forming both micelles at $c \ge$ CMC $\approx$ 10 mM. The micellar solutions have large bulk viscosities, which increase with concentration because of a strong increase of the size of the micelles, finally reaching the gel state at polymer fractions close to 20 mM.[31] The main chemical characteristics of

(12) Aharonson, V.; Andelman, D.; Zilman, A.; Pincus, P. A.; Raphaël, E. *Physica A* **1994**, *204*, 1.
(13) Guiselin, O.; Lee, L. T.; Farnoux, B.; Lapp, A. *J. Chem. Phys.* **1991**, *95*, 4632.
(14) Auroy, P.; Auvrey, L.; Léger, L. *Phys. Rev. Lett.* **1991**, *66*, 719.
(15) Adamuti-Trache, M.; McMullen, W. E.; Douglas, J. F. *J. Chem. Phys.* **1996**, *105*, 4798.
(16) Eisenberg, A.; Lennox, R. B. In *Keynote Lectures in Selected Topics of Polymer Science*; Riande, E., Ed.; CSIC: Madrid, 1995.
(17) Barentin, C.; Muller, P.; Joanny, J. F. *Macromolecules* **1998**, *31*, 2198.
(18) Barentin, C.; Joanny, J. F. *Langmuir* **1999**, *15*, 1802.
(19) Alexander, S. *J. Phys.* **1977**, *38*, 977; **1977**, *38*, 983.
(20) de Gennes, P. G. *Macromolecules* **1980**, *13*, 1069; **1981**, *14*, 1637.
(21) Evers, O. A.; Scheutjens, J. M. H. M.; Fleer, G. E. *Macromolecules* **1990**, *23*, 5221.
(22) Evers, O. A.; Scheutjens, J. M. H. M.; Fleer, G. E. *J. Chem. Soc., Faraday Trans.* **1990**, *86*, 1333.
(23) Marques, C. M.; Joanny, J. F. *Macromolecules* **1989**, *22*, 1454.
(24) Cao, B. H.; Kim, M. W. *Faraday Discuss.* **1994**, *98*, 245.
(25) Richards, R. W.; Rochford, B. R.; Webster, J. R. P. *Faraday Discuss.* **1994**, *98*, 263.
(26) Kuzmenka, D. J.; Granick, S. *Macromolecules* **1988**, *21*, 779; *Polym. Commun.* **1988**, *29*, 64.
(27) Myrvold, R.; Hansen, F. K.; Balinour, B. *J. Colloid Interface Sci.* **1996**, *117*, 27.
(28) Fauré, M. C.; Bassereau, P.; Carignano, M. A.; Szleifer, I.; Gallot, Y.; Andelman, D. *Eur. Phys. J., B* **1998**, *3*, 365.
(29) Johner, A.; Joanny, J. F. *Macromolecules* **1990**, *23*, 5299.
(30) Szleifer, I.; Carignano, M. A. *Adv. Chem. Phys.* **1996**, *XCIV*, 165.
(31) Nyström, B.; Walderhaug, H.; Hansen, F. K. *Faraday Discuss.* **1995**, *101*, 335.

Table 1. Chemical Characteristics of the Two Polymers Used in This Study[a]

				M_w (g/mol)		
polymer	N_A	N_B	N_A/N_B	nominal	LS	M_w/M_n
I	2×76	29	5.24	8350	~9090	1.12
II	2×10	44	0.46	3400	~3600	1.03

[a] The polymerization degree of each block N_i has been calculated from the nominal values of the molecular weight M_w supplied by the manufacturers.

Table 2. Structural and Optical Parameters of the Two Polymers Used in This Study[a]

	$L_{all-trans}$ (Å)		R_F (Å)			n_p	
polymer	A	B	A	B	β	$\sum R_i$	eq 4
I	182.4	147.9	32.3	38.5	1.2	1.454	1.454
II	24.4	222.2	9.6	49.4	5.1	1.450	1.451

[a] A and B refer for the PEO and PPO blocks, respectively.

the two polymers studied are summarized in Table 1. The polydispersity ratios were obtained from GPC analysis using tetrahydrofuran as solvent. The molecular weights were obtained from static light-scattering measurements, showing a good agreement with the nominal values given by the suppliers. Both polymers have a relatively low molecular weight. Pluronic I has lateral PEO blocks longer than the more hydrophobic central PPO block. Pluronic II has a molecular weight approximately half that of Pluronic I, and the terminal blocks are smaller than the central PPO block. The hydrophobic character of these polymers is approximately determined from the ratio N_B/N_A between the polymerization degrees of the blocks. However, a better estimation is the ratio β between the Flory radius R_F of the adsorbing (B) and nonadsorbing (A) blocks:[32]

$$\beta = \frac{R_F^{(B)}}{R_F^{(A)}} = \frac{l_B}{l_A}\left(\frac{N_B}{N_A}\right)^{3/5} \quad (1)$$

where l_i represents the length of a monomeric unit of the block i and N_i its polymerization degree.

By taking the accepted values of the size group l for the PEO and PPO monomers (in the case considered here (PEO) $l_A = 2.4$ Å and (PPO) $l_B = 5.1$ Å), one obtains $l_B/l_A \approx 2.1$. The calculated values of the nominal length of the blocks in the *all−trans* configuration $L_i = N_i l_i$ and the ratio β appear in Table 2. It is thus clear that Pluronic II ($\beta \gg 1$) is more hydrophobic.

To determine precisely the concentration of the solutions, both copolymers were previously vacuum-dried at 80 °C for 24 h. Since these polymers, mainly Pluronic I, show a microcrystalline structure at high temperature, all the solutions were prepared at low temperature (~15 °C) 24 h before the measurements to complete the dissolution process. Afterward, the total absence of microcrystallites and the homogeneity of these aged solutions were checked by observing their optical isotropy by illuminating with a He−Ne laser. This precaution is necessary to prevent possible anomalous reflection effects in the ellipsometry experiments. Double distilled and deionized water from a Milli-Q-RG ultrafiltration system (resistivity > 18 MΩ) was used to prepare the aqueous solutions and the subphase in the case of the spread monolayers. Chloroform solutions were used to spread the monolayers (Carlo Erba), with concentrations of about 10^{-4} M. Spread monolayers were formed by depositing small amounts of these chloroform solutions with a microsyringe (Hamilton) in a Teflon trough containing the subphase. Blank spreading experiments were performed with small amounts of pure chloroform; after its total evaporation, we found values of surface tension and ellipsometric angles identical to those of pure water. Both the aqueous and organic solutions were filtered through a 0.2 μm Teflon membrane (Millipore) before use.

3.b. Surface Tension. The surface tension measurements were performed with a commercial tensiometer Krüss K10 (Germany) by the Pt-Wilhelmy plate method. The experimental accuracy in the measured surface tension γ is ±0.05 mN/m. The samples were contained in a circular Teflon trough (3 cm diameter) and their temperatures measured with a calibrated Pt-100 sensor and maintained constant at $T = 20.0 \pm 0.1$ °C. The evaporation losses were prevented by enclosing this cell in a Plexiglas box with a solvent-saturated atmosphere. This apparatus has been calibrated against different standards (water, ethanol, and acetone), finding good agreement between the values measured and those reported by Jasper.[33]

3.c. Ellipsometry. We have used a Plasmos SD2300 ellipsometer (Germany) with an automated rotating analyzer system. This apparatus operates at the He−Ne wavelength ($\lambda = 632.8$ nm). To maximize the reflected intensity and the polarization sensibility, we have chosen an incidence angle $\theta = 55.00 \pm 0.01°$, close to but slightly higher than the Brewster angle (~53.2°). The liquid samples were contained in a circular Teflon trough with diameter 5 cm. To minimize the evaporation of the solvent and the possible long-time drift due to the contamination of the samples, the trough was enclosed in a Plexiglas box with a small groove to allow the passage of the laser beam. To avoid possible differences between the adsorbed monolayers formed in the different sample containers, the surface-to-volume ratio of the samples studied was always chosen identical in ellipsometric and surface tension experiments ($S/V \approx 1$ cm^{-1}).

This technique allows one to obtain the two ellipsometric angles Ψ and Δ. For an interface between two continuous media with refraction indices n_1 and n_2 (subscript 2 reads to the incident medium) Ψ is related to the change of intensity between the incident and reflected beams. Δ accounts for the phase shift. Both angles are related through[34]

$$e^{i\Delta} \tan \Psi = R_p/R_s = F(n_k) \quad (2)$$

where R_p and R_s represent the overall reflection coefficients for the p- and s-polarizations (parallel and perpendicular to the plane of incidence, respectively).

The variations of the two ellipsometric angles with respect to the values of the *free interface* ($\delta\Psi = \Psi - \Psi_0$ and $\delta\Delta = \Delta - \Delta_0$) are directly related to the refractive index n and thickness d of the film.[34] To estimate n for a composite film, we have followed the approximated model proposed by Yu et al. for inhomogeneous monolayers.[35] In this method, the macroscopic effective value of the film refractive index n is an average of the polymer n_p and water n_w refractive indices, which will be calculated by assuming additivity of the molar refractivities R_i of the film constituents, as given by the Lorentz−Lorenz relationship:

$$R_i = \frac{M_i}{\rho_i}\frac{n_i^2 - 1}{n_i^2 + 2} \quad (3)$$

M_i and ρ_i being the molecular weight and density, respectively.

The method generally accepted to calculate the refractive index n_p for the polymer chain is to add the molar refractivities of the monomer subunits, the end groups, and the bond contributions[36] also via the Lorentz−Lorenz equation given in eq 3. This method has been successfully used for homopolymers and random, graft, or block copolymers with sufficiently low polymerization degree N ($N \leq 1000$).[37] When N is larger, the refractive index approaches a limiting value independent of molecular weight,[37] and can be calculated by using a simple additivity rule:[38]

$$n = \sum_i w_i n_i \quad (4)$$

where w_i is the weight fraction of each block.

(32) Munch, M. R.; Gast, A. P. *Polym. Commun.* **1989**, *30*, 324.

(33) Jasper, J. J. *J. Phys. Chem. Ref. Data* **1972**, *1*, 841.

(34) Azzam, R. M. A.; Basara, N. M. *Ellipsometry and Polarized Light*; North-Holland: Amsterdam, 1992.

(35) Sauer, B. B.; Yu, H.; Yazdanian, M.; Zografi, G.; Kim, M. W. *Macromolecules* **1989**, *22*, 2232.

(36) *Handbook of Chemistry and Physics*, 64th ed.; CRC Press Inc.: Boca Raton, FL, 1983.

(37) Albert, R.; Malone, W. M. *J. Macromol. Sci. Chem.* **1972**, *A6*, 347.

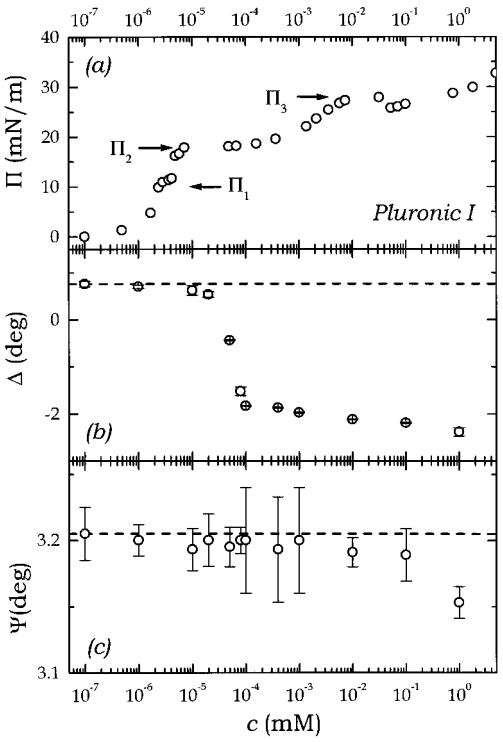

Figure 1. (a) Experimental Π−*c* isotherm at $T = 20.0 \pm 0.1$ °C for the adsorbed monolayers of Pluronic I. Ellipsometric angles (b) Δ and (c) Ψ, measured as a function of the bulk polymer concentration for the same adsorbed monolayers. The dashed lines in (b) and (c) represent the limit values for the pure water.

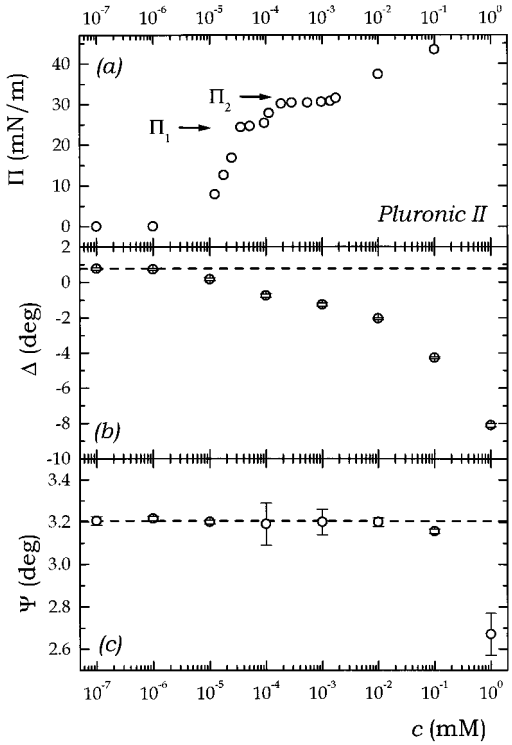

Figure 2. (a) Experimental Π−*c* isotherm at $T = 20.0 \pm 0.1$ °C for the adsorbed monolayers of Pluronic II. Ellipsometric angles (b) Δ and (c) Ψ, measured as a function of the bulk polymer concentration for the same adsorbed monolayers. The dashed lines in (b) and (c) represent the limit values for the pure water.

By using this method, we have calculated the refractive indices for the two polymers used in this study. The values are reported in Table 2. These values are in excellent agreement with those calculated from the additivity rule in eq 4. Furthermore, Ψ depends mainly on the refractive index of the subphase, and only slightly on *d* for large values of *d*. Therefore, in general, one cannot calculate the values of *n* and *d* for a film at the air−water interface. Therefore, we will set reliable values for *n* to estimate the film thickness in the different surface regimes. Depending on the water content of the surface film, *n* must vary between the solvent $n_w = 1.333$ and the pure polymer n_p values. To calculate the reflection coefficients in eq 2, an optical model for the interface must be proposed. An outline of the different models used in this work appears in the Appendix. More precisely, three models, hereinafter, models 1, 2, and 3 will be used in this study. Model 1 accounts for the simpler case of a single and homogeneous polymeric thin film at the air−water interface. Models 2 and 3 reproduce thicker composite films, where a meaningful solvent content (water) is explicitly considered. The refraction index of the film *n* shows, in both cases, intermediate values between those for polymer and water.

4. Experimental Results

4.a. Adsorbed Monolayers. The equilibrium surface tension data γ_{eq} have been taken as the final values of the dynamic curve $\gamma(t)$ at 20.0 ± 0.1 °C, under the assumption that a decrease lower than −0.1 mN/(m h) was a clear signal for total equilibration. Figure 1 collects the static results for Pluronic I. The surface pressure $\Pi = \gamma_0 - \gamma_{eq}$ and the absolute values of the ellipsometric angles Δ and Ψ are represented as a function of the polymer concentration. Different plateaus are observed in the surface pressure (Figure 1a), which could suggest the existence of first-order transitions, $(\partial\Pi/\partial A)_T = 0$. Up to three clear Π = constant regions appear in the isotherm before the CMC, which has been found to be ∼10 mM from viscosity[31] and quasielastic light-scattering[39] measurements. A strong variation in the phase change of the ellipsometric signal, Δ, is also observed for this polymer when the end of the second Π plateau is reached. Usually, the ellipticity of spread monolayers of PEO and other ordinary homopolymers even above collapse is much smaller than the ellipticity reported here.[35] No noticeable ulterior jump is observed at higher concentrations; only a slight decrease at $c \geq 10^{-3}$ mM is noticed. This is probably due to a weak increase in the refraction index of the solutions. The angle Ψ remains almost constant and equal to the solvent value ($\Psi_0 = 3.205 \pm 0.010°$) within the experimental error until $c \approx 0.1$ mM. At this point a weak decrease is observed, nearly coincident to the final decrease in Δ. The decrease of Ψ could be explained by the change in refractive index of the solutions,[34] which occurs above 0.1 mM.

For comparison purposes, a similar study was carried out on the adsorbed monolayers of the PPO-richer Pluronic II. The surface tension and ellipsometric results of the adsorbed monolayers are represented in Figure 2 for this polymer. In this case the first plateau appears also at $c_1 \approx 3 \times 10^{-5}$ mM and $\Pi_1 \approx 25$ mN/m, a value close to the surface pressure at saturation in the pure PPO monolayer.[40] Above c_1 an additional Π increment is observed until a second plateau at $\Pi_2 \approx 30$ mN/m. The third Π increment and the subsequent plateau were not observed in this case at higher concentrations due to the high viscosity of the solutions, which posed problems in the Π measurements by the Wilhelmy method. Nevertheless, the ellipsometric data show a significant difference from

(38) Brandrup, J.; Immergut, E. H. *Polymer Handbook*; Wiley: New York, 1989.

(39) García, M.; Monroy, F.; Ortega, F.; Rubio, R. G. Unpublished results.

(40) Fu, S.; Li, W.; Gu, T. *Colloids Surf. A* **1987**, *25*, 167.

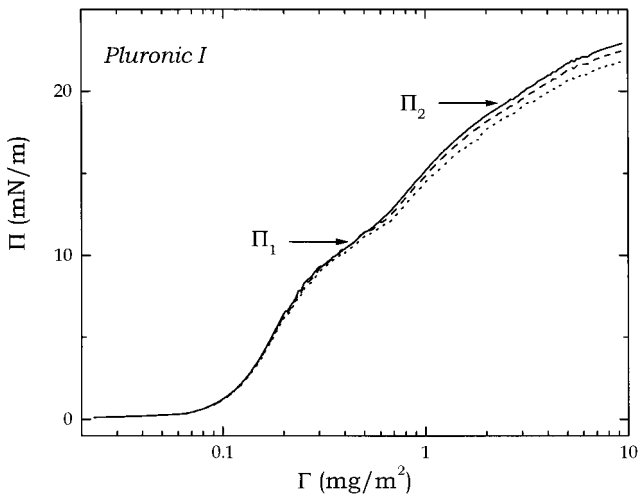

Figure 3. Experimental Π−Γ isotherm for the spread monolayer of Pluronic I at $T = 20.0 \pm 0.5$ °C. This curve has been obtained by symmetric continuous compression in a Langmuir trough at different velocities of the barriers v_C expressed in Å²/monomer/min: (—) 0.75; (- - -) 0.50; (···) 0.25.

those of Pluronic I. The Δ decrease at Π_2 is approximately equal for both polymers ($\Delta \approx -2°$). However, a smooth decrease in Δ is observed in the PPO-rich Pluronic II monolayer until $c_2 \approx 2 \times 10^{-4}$ mM (see Figure 2b), which contrasts with the sharp jump found for Pluronic I (see Figure 1). Increasing further the concentration of Pluronic II in this last copolymer causes an additional decrease to $\delta\Delta \approx -8°$, followed by a strong decrease of Ψ at $c > 0.1$ mM. These observations seem to support the sketch of conformational transitions accompanied by film thickening, but a more detailed analysis of the surface properties is necessary to clarify the mechanism for molecular rearrangement at the interface.

4.b. Spreading Monolayers. We have found that the adsorption kinetics for these systems is extremely slow for sufficiently low bulk concentrations ($c \leq 10^{-4}$ mM). As a consequence, compression experiments on spread monolayers can be carried out. If a spread monolayer is deposited on the surface of pure water at an initial surface concentration corresponding to a bidimensional gas, and if the time necessary to initiate the surface-to-bulk dissolution process τ_D is long enough, such a monolayer may be considered as insoluble (Langmuir monolayer), at least for times $\tau < \tau_D$. Under these conditions the Π−A isotherms should be equivalent to those found for the adsorbed monolayers (provided that the time of the measurements is small compared with the hours, even days, necessary to complete the diffusive transport).

To study the equivalence of these quasi-Langmuir monolayers with the adsorbed ones or Gibbs monolayers, a small quantity of Pluronic I was spread at the air−water interface from a chloroform solution. To check for phase transitions, this experiment was performed in a Langmuir trough equipped with a Brewster angle microscope (BAM utility at CRPP, France). Figure 3 shows the Π−Γ isotherms for a Pluronic I monolayer spread at 20 ± 1 °C. The initial surface concentration was fixed at $\Gamma = 0.023$ mg/m² (~60 000 Å²/molecule and $\Pi \approx 0.3$ mN/m), which would correspond to the gas state. Experiments at different compression velocities v_C were carried out. As can be observed, the more diluted part of the isotherms ($\Gamma \leq 0.4$ mg/m²) is independent of v_C. In this regime, Π shows a strong increase with the surface concentration until a value close to ~0.3 mg/m² is reached. At this point, a noticeable change in the curvature of the Π−Γ curve is observed, and a pseudoplateau appears at $\Gamma_1 \approx 0.45$ mg/m² and $\Pi_1 \approx 11.0$ mN/m. This pressure plateau is also observed in the adsorption isotherm of Figure 1a, and close to the surface pressure at which the pure-PEO monolayers reach their saturation plateau.[26,41] By using the data in Table 1, one finds a value $A_1 \approx 19.5$ Å²/unit, for the area per monomer at this surface concentration, which is in good agreement with the averaged PEO−PPO monomer size. Therefore, it can be considered that at this point all the adsorption sites in the surface are occupied by monomeric units, with all polymer chains lying parallel to the surface. Further compression causes an additional increase of the surface pressure in a way similar to that of the adsorption isotherm (see Figure 1a), and the previous observations in alkyl end-capped monolayers formed by spreading,[17] or adsorption from the solution.[42] However, above this point, the Π−Γ isotherm shows increasing Π values at larger v_C and hysteresis in compression−expansion cycles, which indicates either dissolution of the polymer in the bulk[26,27] or internal rearrangement of the film.[43] Similar observations have been previously carried out by Joanny et al.[17] in modified PEOs with insoluble alkyl ends. In this work, the compression isotherms also show long-time stability and reversibility before the first plateau at Γ_1.

A morphological characterization has been tentatively performed by observing the monolayer textures by Brewster angle microscopy (BAM). The BAM images of the monolayer of Pluronic I show a homogeneous background with increasing brightness until Γ_1 is reached. At this moment, small brighter circular patches begin to appear. The maximum resolution of the BAM instrument was insufficient for a precise determination of the size of these patches. They appear as 2−5 pixel bright circular domains in the digitized images, allowing us to give a size estimation around 1−2 μm. Upon compression of the monolayer, the size of these domains remains essentially constant, but their number increases.

At the second pseudoplateau in the isotherm ($\Gamma_2 \approx 2.5$ mg/m² and $\Pi_2 \approx 19$ mN/m), the BAM image becomes more homogeneous through a process of overlapping of the bright domains. The resolution of the BAM instrument was always insufficient to give well-defined images. However, measurements of the optical reflectivity averaged over the whole field of view revealed a noticeable increase of the refraction index of the film at $\Gamma \geq 2$ mg/m². It is worth noting that, at this surface concentration, $\Pi \approx 19$ mN/m, which is approximately the same surface pressure of the second Π plateau, and of the Δ jump in Figure 1b. Similar morphologies were observed by BAM in the adsorbed monolayers at different bulk concentrations in the first ($c_1 = 3 \times 10^{-6}$ mM) and second ($c_2 = 6 \times 10^{-5}$ mM) plateaus in Figure 1a. Adsorption effects were also observed since the small bright domains appear only 10−15 min after surface aspiration with a Pasteur pipet.

Since biphasic behavior has been inferred from the BAM characterization, the observed Π plateaus might correspond to first-order phase transitions, characterized by $(\partial\Pi/\partial A)_T = 0$. The nature of the phases still remains unknown, but it became evident that the granular phase is denser than the continuous one, which becomes a minority at high surface pressure ($\Pi \geq 19$ mN/m). Since the ellipsometric thickness proportional to $\delta\Delta$ grows suddenly at this point, the second phase is probably a brush of PEO blocks swollen by water, and grafted to the

(41) Sauer, B. B.; Yu, H. *Macromolecules* **1989**, *22*, 786.
(42) Kim, M. W.; Cao, B. H. *Europhys. Lett.* **1993**, *24*, 229.
(43) Monroy, F.; Ortega, F.; Rubio, R. G. *Phys. Rev. E* **1998**, *58*, 7629.

interface by the more hydrophobic central PPO blocks. This microscopic sketch is supported by the comparison of the surface pressure of equivalent states in the Gibbs or Langmuir monolayers, with plateaus at $\Pi_1 \approx 11$ mN/m and $\Pi_2 \approx 19$ mN/m in both isotherms. The first corresponds to an area per monomer compatible with a saturated thin monolayer made of copolymer chains parallel to the surface plane. Obviously, further compression will cause either chain dissolution or the suggested conformational change with increasing thickness. However, the additional Π increase with respect to the pure PEO monolayer and the simultaneous manifestation of a biphasic morphology is compatible with the second hypothesis.

5. Discussion

5.a. Adsorbed Monolayers and Gibbs Equation. The $\Pi-c$ isotherms of the adsorbed monolayers might also be analyzed with the Gibbs equation for adsorption from a diluted solution:

$$\Gamma(c) = -\frac{a}{RT}\frac{\mathrm{d}\gamma}{\mathrm{d}a} \approx -\frac{c}{RT}\frac{\mathrm{d}\gamma}{\mathrm{d}c} \approx -\frac{1}{RT}\frac{\mathrm{d}\gamma}{\mathrm{d}\ln c} \qquad (5)$$

where a and c are the activity coefficient and the molar concentration, respectively.

Since the solutions are diluted ($c \ll 1$ mM), ideal bulk behavior can be assumed, and in this case, $a \approx c$. The surface excess concentrations $\Gamma(c)$ can be obtained as a function of the bulk concentration only if surface or bulk aggregates are not present. Here, there are two different monomeric units (A = PEO and B = PPO), and the Gibbs equation can be written as

$$\mathrm{d}\gamma = -RT[\Gamma_A\, \mathrm{d}\ln c_A + \Gamma_B\, \mathrm{d}\ln c_B] \qquad (6)$$

The bulk concentrations of both types of monomers are related to the total polymer concentration c, $c_A = N_A c$ and $c_B = N_B c$. The total surface adsorption is $\Gamma = \Gamma_A + \Gamma_B$, and if all the monomers of an adsorbed chain are at the interface, $\Gamma = (2N_A + N_B)\Gamma_{chains}$. In this case

$$\mathrm{d}\gamma = -RT(2N_A + N_B)\Gamma_{chain}\, \mathrm{d}\ln c \qquad (7)$$

The slope $\mathrm{d}\gamma/\mathrm{d}\ln c$ for Pluronic I has been calculated from the $\Pi-c$ isotherms, leading to the values of surface adsorption, Γ_{chain}, shown in Figure 4 for different Π values. For the sake of comparison, the experimental $\Pi-\Gamma$ isotherm obtained by compression of the spread monolayer is also shown in the figure. There is an excellent agreement between the calculated adsorption excess and the surface concentration in the range $\Pi < 10-12$ mN/m. This supports the validity of the Gibbs equation and the thermodynamic equivalence of adsorbed and compressed surface states with equal surface pressures. Discrepancies are found for $\Pi > \Pi_1 \approx 12$ mN/m, consistent with the assumptions of brush formation. If there would be surface saturation at the first plateau ($\Pi_1 \approx 11$ mN/m), one would have a thin homogeneous polymer layer with refractive index $n = n_p = 1.454$. Ellipsometry gives $\delta\Delta = -0.23 \pm 0.06°$ at this point, and Drude's equation for the single-layer model (see the Appendix) leads to $d = 1.5 \pm 0.3$ Å. This value is lower than the one found by Yu et al.[35] for the saturated monolayer of POE, 3.4 ± 0.2 Å. However, we should stress that our value was calculated by neglecting the thermally induced roughness, which gives a contribution of opposite sign. The real value of d is therefore slightly larger than 1.5 Å, but in any case compatible with the idea of a thin monolayer.

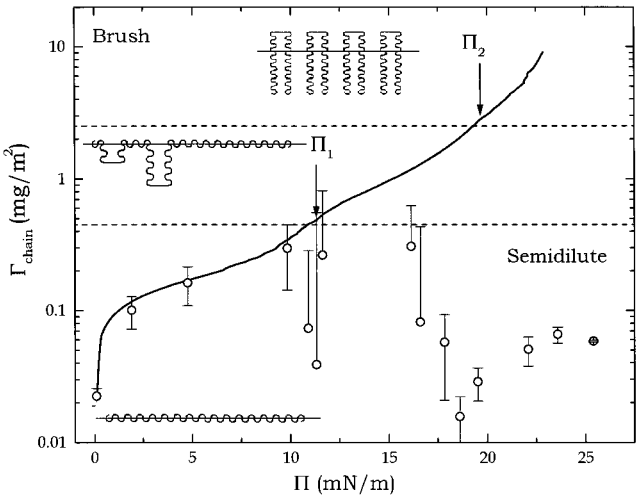

Figure 4. Comparison between the $\Gamma-\Pi$ data for spread and adsorbed monolayers of Pluronic I. The adsorbed amount $\Gamma(\Pi)$ has been obtained from the isotherm in Figure 1 by using the Gibbs equation (eq 17). Full adsorption behavior is only possible at $\Pi \le \Pi_1$. Further compression causes partial dissolution of the polymer in water, and finally a complete brush is formed at $\Pi > \Pi_2$.

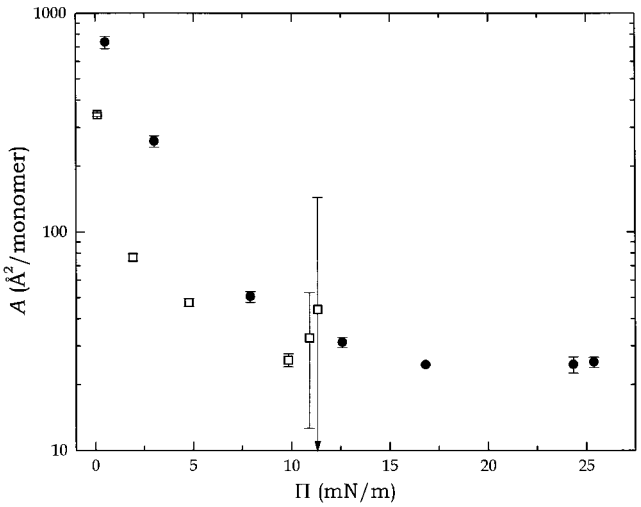

Figure 5. Monomeric area as a function of surface pressure in the full adsorption regime $\Gamma \le \Gamma^{**}$. These values have been calculated from the Gibbs equation (eq 17) for both polymers: (□) Pluronic I and (●) Pluronic II.

A similar calculation based on the Gibbs equation has been performed for Pluronic II, obtaining $\Gamma_1 \approx 0.14$ mg/m^2 at the first plateau $\Pi_1 \approx 25$ mN/m, in good agreement with the accepted values for film saturation in pure PPO monolayers.[40] The calculated value of the ellipsometric thickness at this saturation point is $d = 5.5 \pm 0.5$ Å, noticeably higher than the value found for Pluronic I, but also consistent with the expected values for a thin monolayer.[35] The differences with Pluronic I could be related to a weak thickening of this adsorbed monolayer by accommodation of the more hydrophobic PPO block in the air.

For the sake of comparison, Figure 5 shows the area per monomeric unit A, as obtained from the Gibbs adsorption equation for both polymers at $\Pi \le \Pi_1$. A strong decrease in A with increasing surface pressure is observed in both cases, reaching a saturation limit value at Π_1. The saturation areas are equal for both polymers within the experimental accuracy, $A_1^{I} \approx A_1^{II} \approx 26 \pm 1$ Å^2/monomer, being approximately twice the size of a monomeric EO

unit, ~13 Å^2; however, the plateau pressure Π_1 is ~11 mN/m for Pluronic I and ~25 mN/m for Pluronic II. Moreover, at lower surface coverage, in the diluted and semidiluted regimes, the area occupied per monomer at a given pressure is noticeably higher for Pluronic II.

Similar values for monomer area at saturation $A_1 \approx 26$ Å^2 have been reported for partially insoluble polyester−poly(ethylene oxide) (PE−PEO−PE) triblock copolymer monolayers at saturation.[27] In that work a kink in the isotherms and an additional Π increase were also detected at surface concentrations higher than the saturation value. The authors claim that, in such a situation, the central PEO block is displaced away from the interface into the water subphase, with only two EO monomers or two vertically orientated PEO chains (each with an area of about 13 Å^2) at the interface.[27] The qualitative configurational image shown in Figure 4 could be proposed for both adsorbed and spread monolayers (see section 5.b). For $\Gamma < \Gamma_1$, EO or PO monomers are all adsorbed. For $\Gamma_1 < \Gamma < \Gamma_2$, the lateral PEO block will be partially stretched out from the interface into the aqueous phase, while a compressed PPO phase rests at the interface. As suggested from the highly ordered structures observed in bulk crystalline polymers,[44] the central PPO blocks would adopt a folded chain structure as illustrated in Figure 4. Further compression of this structure at $\Gamma > \Gamma_2$ would also stretch the PPO blocks from the interface to the air phase.

5.b. Spreading Monolayers. As has been discussed in section 2, several surface concentration regimes are *a priori* possible. Scaling behavior of the surface properties with Γ is useful to distinguish between the different surface states.

5.b.1. Dilute and Semidilute Regimes. In the dilute and semidilute regimes one expects

$$\Pi_a = \alpha\Gamma^y \qquad (8)$$

where $y = 1$ in the dilute regime (ideal gas law) and $y = 2\nu/2\nu - 1$ in the semidilute regime; ν is the Flory exponent and takes values between 0.77 and 0.57, leading to $y = 2.8-8.1$ for good and Θ solvent conditions, respectively.

The inset in Figure 6 shows the log−log representation of the experimental isotherm for Pluronic I, obtained from the experimental data in Figure 3. At $\Gamma^* = 0.065$ mg/m^2 a net change from gas behavior ($y = 0.992 \pm 0.007$) to a semidiluted bidimensional solution in a good solvent ($y = 2.75 \pm 0.02$) is observed. The molecular area at Γ^*, $A^* \approx$ 20 000 Å^2/chain (~110 Å^2/monomer), is lower than the theoretical random-coil overlapping area, 33 400 Å^2/chain, obtained from the Flory radius $A^* \approx \pi R_F^2$ (with $R_F = lN^{3/5}$), which has been calculated by adding the individual contributions of the blocks. Further compression forces the chains to overlap laterally in the semidilute regime ($\Gamma^* \le \Gamma \le \Gamma^{**}$) until the multiple cross-linking state or concentrated regime at $\Gamma > \Gamma^{**}$.

5.b.2. Concentrated Regime. In monolayers of fully insoluble polymeric materials, the scarcity of adsorption sites at $\Gamma \ge \Gamma^{**}$ causes the extreme condensation of the 2D-confined material, and the monolayer becomes stiffer, and finally collapses, with the appearance of tridimensional aggregates. Several paths for tridimensional arrangement can be proposed: (A) Collapse, usually found in insoluble monomeric surfactants and homopolymers when the surface concentration exceeds the limiting value given by the volume excluded by one monomer. Since any additional adsorbate−interface interaction is established

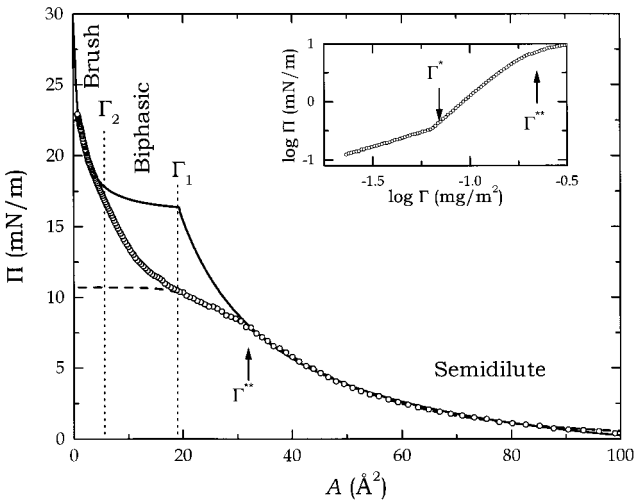

Figure 6. Surface pressure as a function of the area per monomer for the spread monolayer of Pluronic I at $T = 20.0 \pm 0.5$ °C: (○) experimental values obtained from the data in Figure 3; (—) theoretical prediction obtained from scaling behavior (eq 6) in the full adsorption regime ($\Gamma \le \Gamma^{**}$) and the thermodynamic mean theory for polymer brushes (eq 8) at $\Gamma \ge \Gamma_2$. The crossover between the two regimes is predicted at $\Gamma = \Gamma_1$, where biphasic behavior stars, as derived from the BAM observations. The log−log representation in the inset gives the different scaling regimes in the full adsorption branch of the isotherm: quasi-ideal gas behavior at $\Gamma \le \Gamma^*$; a semidiluted 2D solution in a good solvent at $\Gamma^* \le \Gamma \le \Gamma^{**}$; a concentrated regime at $\Gamma \ge \Gamma^{**}$.

in further compressing a collapsed monolayer, Π must remain constant at $\Gamma > \Gamma^{**}$, which is not true in our case. (B) Brushing and (C) 2D Micellization. Both are tridimensional self-assembling processes, driven by hydrophobicity differences between blocks in the polymer chain. If there are hydrophilic blocks in the chain, a partial solubilization of the surface excess in the aqueous subphase could occur, while the hydrophobic segments remain linked to the interface. Such a structure is called a polymer brush. However, if the hydrophobic blocks are long enough, the entropic increase attained in forming a lens of hydrophobic segments is larger than the hydration energy; then 2D micellization occurs. The first structure or *brush* phase can be pictured as a thicker planar layer of swollen polymer, while the *2D micellar* phase is composed of a highly curved lens, made of hydrophobic segments aggregated (micellar core) and hydrophilic arms lying adsorbed at the interface in a near-plane conformation. However, 2D micelles have been observed,[45] only when the hydrophobicity and the length of the core-forming block are much higher than those of the slightly hydrophobic and oligomeric PPO blocks of the copolymers considered here. Moreover, since micellization is an entropy-driven process promoted by the hydrophobic blocks, it is always characterized by a negative temperature coefficient of the surface pressure, $(\partial\Pi/\partial T)_\Gamma < 0$.[16] This thermal behavior is contrary to our experimental findings,[46] and to that expected for a brushing process, which is essentially a solubilization process driven by the hydration energy of the more hydrophilic groups in the aqueous subphase.[17,18,47] In fact, positive values of this coefficient temperature, $(\partial\Pi/\partial T)_\Gamma > 0$, have been systematically found for the small slightly hydrophobic copolymers considered in this study.[46]

(44) Sperling, L. H. *Introduction to Physical Polymer Science*; Wiley-Interscience: New York, 1986.

(45) Zhu, J.; Eisenberg, A.; Lennox, R. B. *Macromolecules* **1992**, *25*, 6547; **1992**, *25*, 6556.

(46) As expected for 3D gases, the surface pressure increases monotonically with temperature for the monolayers of both polymers studied here (unpublished results).

(47) Rother, G.; Findenegg, G. H. *Colloid Polym. Sci.* **1998**, *276*, 496.

Consequently, although additional morphological and structural information is lacking to elucidate the true molecular arrangement after the thickening transition observed at $\Gamma > \Gamma^{**}$, the planar structure of the brush seems *a priori* more favorable, in our case, than micellization.

As has been pointed out by Joanny et al.,[17,18] an equilibrium between two kinds of polymer configurations is possible in partially soluble brushing systems at $\Gamma \geq \Gamma_1 \geq \Gamma^{**}$. At surface concentration well above Γ^{**} the 2D-confined material is strongly compressed, but if the adsorption energy is weak ($\sim k_B T$), some polymer chains previously adsorbed at the interface are now stretched out at $\Gamma = \Gamma_1$, dangling into the aqueous phase. In this state an additional contribution to the surface pressure from the grafted chains Π_b must be taken into account:[48]

$$\Pi(\Gamma) = \Pi_a(\Gamma_a) + \Pi_b(\Gamma_b) \tag{9}$$

In this coexistence regime, ideal mixing between grafted and fully adsorbed chains has been assumed. From a self-consistent mean field approach, Milner et al.[49] have calculated the contribution of the brush by assuming both high conformational stability of the stretched polymer chains and intermolecular interactions through a mean field potential, proportional to the square of the local concentration in the brush $V(z) = wc(z)^2$. This is in principle valid only in a Θ solvent, but for simplicity we will adopt this approach here, which is the only one currently available and easily applicable to this regime.[17,18] Π_b is then given by[17,49]

$$\Pi_b(\Gamma_b) = k_B T \left(\frac{6w}{a^2}\right)^{1/2} \frac{1}{N} \Gamma_b^{\,2} \tag{10}$$

where the nonuniversal amplitude factor $(6w/a^2)^{1/2}$ takes into account the interactions between tails in this brush regime.

From Figure 6, the end of the semidilute regime has been determined around $\Gamma^{**} \approx 0.20$ mg/m^2 (monomeric area $\sim$38 Å^2). Further compression above Γ^{**} could produce first a concentrated monolayer regime followed by a coexistence of fully adsorbed (a) and grafted (b) material. In the coexistence region, the equilibrium conditions are the equality of the chemical potentials and the mass balance:

$$\mu_a(\Gamma_a) = \mu_b(\Gamma_b) \tag{11}$$

$$\Gamma_a + \Gamma_b = \Gamma \tag{12}$$

By integrating the partial contributions to the total surface pressure Π_a for the fully adsorbed material (eq 8) and Π_b for the grafted chains (eq 10), one obtains the following expressions for the chemical potential per monomeric unit:[17]

$$\mu_a(\Gamma_a) = (3/2)\alpha N \Gamma_a^{\,2} - eN \tag{13}$$

$$\mu_b(\Gamma_b) = 2k_B T \left(\frac{6w}{a^2}\right)^{1/2} \Gamma_b \tag{14}$$

where e is the adsorption energy per monomer.

In the coexistence region $\mu_a = \mu_b$ and finally, from the equilibrium conditions (eqs 11 and 12), an additional constraint is obtained:[17]

$$\Gamma_b = \frac{3/2\alpha\Gamma_a^{\,2} - e}{2k_B T(6w/a^2)^{1/2}} N \tag{15}$$

From this equation one sees that polymer grafting increases with the adsorption density Γ_a and decreases as the adsorption energy increases. Since Γ_b is necessarily positive, the lower concentration limit of the coexistence region is given by[17]

$$e = (3/2)\alpha\Gamma_1^{\,2} \tag{16}$$

We have fitted the data of the compression isotherm (see also Figure 3) to this model in the semidiluted regime (eq 8) and diluted brush regime (eqs 9 and 10). The theoretical curve in Figure 6 does not fit the vicinity of $\Gamma_1 \approx 0.10$ mg/m^2, as expected, but accurately predicts the semidilute regime ($\Gamma < \Gamma^{**}$) and the brush regime above $\Gamma_2 \approx 0.34$ mg/m^2.

From these fits one obtains $\alpha = (2.0 \pm 0.4) \times 10^8$ N m^5/g^3, $e \approx 0.9\ k_B T$, and $(6w/a^2)^{1/2} \approx 53$ Å^2/monomer, values slightly higher than those found by Joanny et al. for telechelic PEO: $e \approx 0.6\ k_B T$ and $(6w/\alpha^2)^{1/2} \approx 40$ Å^2/monomer.[17] The triblock copolymer studied here contains a more hydrophobic PPO block, with a higher surface activity than the smaller EO segments; hence, a higher adsorption energy is expected. The characteristic distance for tail−tail interaction, approximately given by the $(6w/a^2)^{1/2}$ factor, is also expected to be larger since grafting is due to the more hydrophobic central PPO blocks, larger than the small lateral alkyl chains in the end-capped PEO.[17]

5.c. Ellipsometric Thickness. It seems clear that Π_1 represents the limit of saturation of the full adsorption regime. Thus, it seems reasonable to analyze the ellipsometric data at $\Pi \leq \Pi_1$ in terms of a two-component thin single-layer model with an asymptotic $n = n_p$ value at saturation (see model 1 in the Appendix). At $\Pi_1 > \Pi > \Pi_2$ the situation is more complex due to the coexistence of the polymer brush with fully adsorbed chains, while at $\Pi > \Pi_2$ only a compact brush should exist. In this case the film might be modeled as a thick homogeneous film made of polymeric cylinders oriented perpendicular to the interface (model 2) or more realistically by a two-layer model. The upper layer, in contact with air, would be mainly constituted by the PPO anchoring blocks, while the lower one is a thick layer of swollen PEO (model 3). In such a structure there is a large quantity of water filling the free space of the compact packing. For a precise evaluation of the refraction index of the brush structure for the two copolymers, the cubic packing pictured in Figure 7 has been assumed. The spherical cores are made of melt polymer, while the surrounding space in the cubic box is filled by water. The values of the refractive index of such brushes have been calculated by using a volume fraction average of the molar refractivities. By applying the Lorentz−Lorenz relationship (see the Appendix for details) for the rectangular lattice of Figure 7, one obtains $n_I = 1.395$ and $n_{II} = 1.393$ for the adsorbed brushes of Pluronic I and II, respectively. For the sake of comparison, we have calculated the increase in the ellipsometric angle as a function of the total film thickness for the three interfacial models, *i.e.*, model 1, uniform thin polymer film with $n = n_p$; model 2, thicker swollen brush modeled as a single layer with a volume fraction averaged refraction index

(48) Motschmann, H.; Stamm, M. *Macromolecules* **1991**, *24*, 3681.
(49) Milner, S. T.; Witten, T. A.; Cates, M. E. *Macromolecules* **1988**, *21*, 2610.
(50) Asnacios, A.; Langevin, D.; Argillier, J. F. *Macromolecules* **1996**, *29*, 7412.

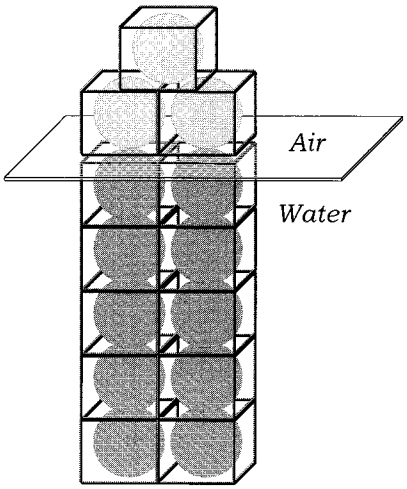

Figure 7. Microscopic sketch of a polymer chain bigrafted at the air−water interface in a good solvent. The rectangular lattice model represented below has been used to calculate the solvent content in the brush.

(PPO/PEO/water); and model 3, or two-layer model, with an upper thin film of melt PPO and a subjacent swollen brush made of PEO blocks. The details of the calculations for the three models are given in the Appendix. The results of the simulations, performed by evaluation of the total reflection coefficients via the Fresnel relationships for each interface,[34,51] and the comparison with the experimental data for Pluronic I are shown in Figure 8. One can easily observe that the uniform melt model ($n = n_p$) yields a smaller thickness at a given $\delta\Delta$ than the swollen film models ($n_w < n < n_p$). The variation in ellipsometric angles calculated from both models 2 and 3 is almost nonexistent at small thickness, while a weak difference appears at $d > 50$ Å. This confirms the small influence that a formal separation of the PPO and PEO layers (with very close refraction indices) has on the optical properties of the interface. However, as shown in Figure 8a, the two swollen brush models (one or two layers) yield a weak, but significant, decrease in $\delta\Psi$ as the thickness increases. This is similar to the behavior observed experimentally on increasing the bulk concentration. These features seem to corroborate the thickening character, with PEO solubilization (n decreasing with respect to n_p), of the observed jump in the ellipsometric angle Δ at $\Gamma \geq \Gamma_2$. At this point, a swollen brush with an intermediate refraction index (intermediate between the values for the polymer and water) might appear.

The interfacial thickness calculated from the uniform polymer melt model 1 and the two-layer model 3 (2 Å uniform upper PPO layer + PEO brush in water) has been represented in Figure 9 for the two copolymers studied. For Pluronic I, a strong increase of the ellipsometric angle is observed at $c > c_2$, independent of the model used. If the fully adsorbed thin layer model is correct, and if polymer brushes are not formed, a 3D collapse process would be expected. Then the data would indicate that above c_2 there is a sudden packing of 8−10 layers of horizontal polymer chains, which does not seem a likely possibility. If a polymer brush were formed ($n_p > n > n_w$), a strong increase of the ellipsometric thickness would be expected. Thickness values of ~33 and ~65 Å for Pluronic I and II, respectively, are derived from model 2. A reliable confirmation for this hypothesis emerges from the estimation of the thickness of the polymer brush, $d \approx \Gamma/\rho$, where ρ is the bulk density. By using the value of Γ for Pluronic I at $\Pi \approx \Pi_2$ ($\Gamma_2 \approx 3$ mg/m^2; see Figure 3), where the brush is expected to be fully built and $\rho \approx 1$ g/cm^3, we get a d value close to the maximum value of the ellipsometric thickness.

5.d. Tentative Interfacial Model. Let us also consider the theoretical predictions for the thickness of polymer brushes. From a microscopic point of view, the polymer brush can be considered as a close packing of subunits, called *blobs*, whose size is on the order of the mean distance between tails (see Figure 7). From the scaling description of such a complete monodisperse brush in a good solvent, the volume fraction of polymer can be estimated by[19,20]

$$\phi_p \approx \sigma^{2/3} \tag{17}$$

where σ is the grafting density.

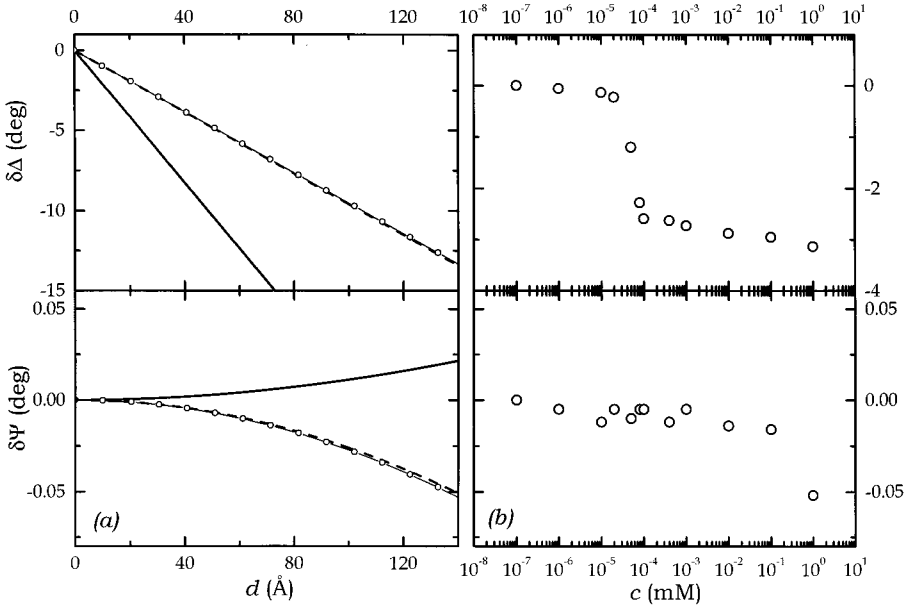

Figure 8. (a) Calculated incremental ellipsometric angles for the air−water interface with a polymeric film of thickness d: (—) single uniform layer of the melt polymer; (- - -) single layer composed of a swollen brush with refractive index as given by eq 18; (○) stratified film with two layers (top, 5 Å thickness uniform film of melt PPO; bottom, swollen PEO brush). (b) Comparison with the experimental increments $\delta\Delta$ and $\delta\Psi$ for Pluronic I obtained from the data in Figure 1.

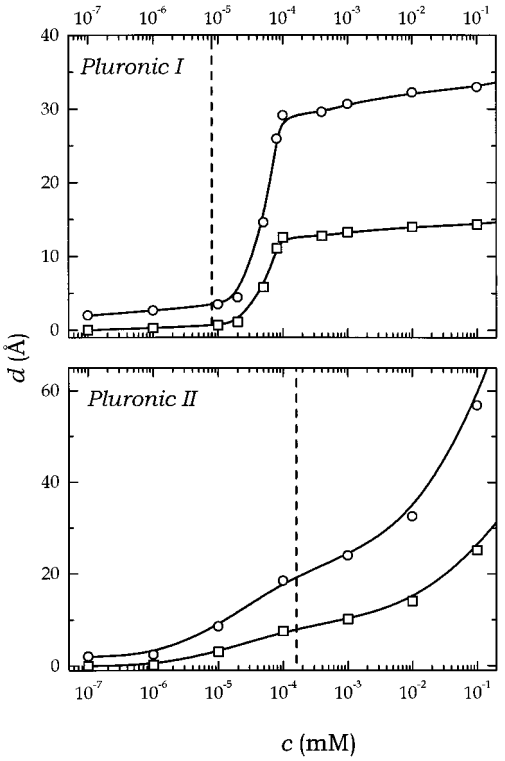

Figure 9. Ellipsometric thickness d of the adsorbed monolayers of both polymers, calculated from the ellipticities in Figures 1b and 2b by using Drude's equation for the limiting behaviors: (□) thin full adsorbed film with $n = n_p$ and (○) thick swollen brush.

In this complete brush regime, σ can be assumed to be equal to the monomer density at saturation in the full adsorption regime, $\sigma = l^2/A_\infty$, where l is the monomer length. If one considers grafting to occur by the more hydrophilic EO segment,[27] $l \approx 2.4$ Å, and a grafting density of $\sigma \approx 0.23$ is obtained by assuming $A_\infty \approx 26$ Å^2/monomer, equal for both polymers (see the discussion in section 5.a). Finally, the average volume fraction of the polymer in the brush can be obtained from eq 17, resulting in $\phi_p \approx 0.4$, a value compatible but slightly lower than the polymer fraction, $\phi_p \approx 0.5$, calculated from the geometric *hard sphere* model in Figure 7. This suggests that the polymer brush is really more swollen than a compact blobs model. Consequently, noticeably higher values of the ellipsometric thickness d could then be obtained from the experimental $\delta\Delta$ values, confirming the hypothesis for brush formation.

The total thickness L of such a swollen complete brush in a good solvent can be estimated by[19,20]

$$L \approx Nl\sigma^{1/3} = Nl\phi_p^{1/2} \qquad (18)$$

By setting $\phi_p \approx 0.4$, the values of L are calculated from this approach, 163.4 and 85.6 Å for Pluronic I and II, respectively. These values are higher than those calculated from R_F (see Table 3), but much smaller than the chain length obtained for the *all−trans* conformation in the ideal folded cylinder configuration $L \approx L_A + {}^1/_2L_B$. This is expected for a polymer chain stretched due to the confinement induced by the brush.

As can be seen in Table 3, the hydrodynamic dimensions obtained from this approach are systematically higher than the values calculated from the ellipsometric thickness, pointing out again the high water content of the brush. To quantitatively illustrate this effect, a deviation from the ideal folding of the adsorbing central PPO block, resulting in an inverted-V structure, can be considered. This effect is displayed in Figure 10 where the proposed microscopic geometry has been represented. The calculated values of the aperture angle ϕ, $\cos(\phi/2) = d/L$, obtained by using the data in Table 3, show a clear asymptotic limit $\phi = 180°$ at $c \to 0$, which corresponds to the horizontal full adsorption conformation at low surface occupation. A weak flexion angle of the lateral blocks is predicted for Pluronic I, $\phi_{max} \approx 140°$, which seems compatible with the symmetry of this chain with three blocks approximately equal in size. However, because of the larger size of the more hydrophobic central PPO block in Pluronic II, this polymer can easily accommodate the PPO surface excess in the air phase, resulting in a much higher flexion of the chain by its center, $\phi_{max} \leq 40°$, in the more concentrated regime.

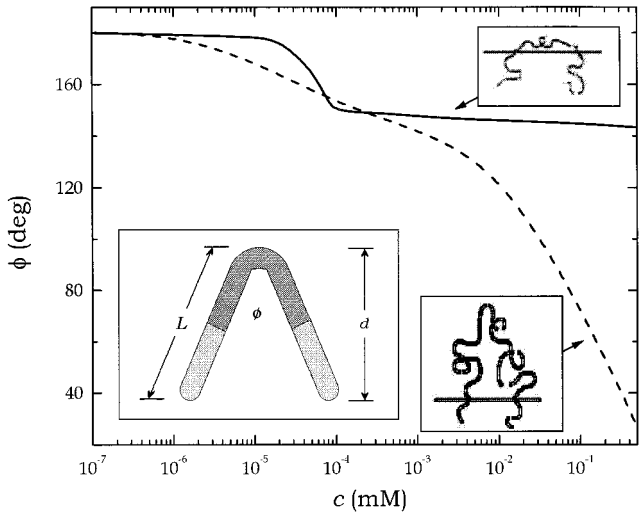

Figure 10. Aperture angle ϕ of the folded-by-the-center ideal structure of triblock copolymer chains grafted at the air−water interface for (—) Pluronic I and (- - -) Pluronic II. This calculation has been performed by comparison of the ellipsometric thickness in Figure 8 with the molecular dimensions of the ideal perpendicularly grafted brush configuration, obtained from the scaling theory in a good solvent.

Table 3. Calculated Values of the Brush Thickness from the Different Theoretical Approaches and from the Experimental Variation of the Ellipsometric Angle $\delta\Delta$

	interfacial thickness (Å)			
polymer	*all−trans*	hydrodyn	Flory	d_{ellip}
I	∼256	∼163	∼103	∼33
II	∼136	∼86	∼69	∼65

6. Conclusions

Equilibrium surface tension and ellipsometric measurements of adsorbed and spread monolayers of symmetric triblock PEO−PPO−PEO polymers indicate singular behavior at saturation of the adsorption sites in the monolayer; an additional Π increase followed by a strong increase of the ellipsometric thickness of the film is observed at higher concentrations. The equivalence between adsorbed and spread surface states with equal surface pressure in the full adsorption regime has been established by using the Gibbs equation.

At least three surface states have been found from the scaling analysis of the experimental isotherms and from the ellipsometric data, *e.g.*, initially, the polymer chains lie extended in a horizontal configuration, maintaining

(51) Tompkins, H. G. *A User's Guide to Ellipsometry*; Academic Press: San Diego, 1993.

all their monomers adsorbed at the interface, while at $\Pi > \Pi_1$ the more hydrophilic PEO blocks are stretched out from the interface to the water subphase because of the scarcity of adsorption sites, leading to a diluted polymer brush. Finally, at $\Pi > \Pi_2$ a complete brush appears.

In the full adsorption state at $\Pi < \Pi_1$, three concentration regimes have been pointed out: a dilute regime with ideal gas behavior, which ends when the fully adsorbed horizontal polymer chains begin to overlap at $\Gamma = \Gamma^*$, a lateral overlapping or semidilute regime in a good solvent with the polymer chains in the extended conformation, and, finally, the concentrated regime at $\Gamma > \Gamma^{**}$ where the high condensation in the 2D plane leads the chains to stretch their more hydrophilic lateral PEO blocks into the aqueous phase. At this point, the brush phase forms.

Although both the decreasing trend of $\Delta\Psi$ with increasing surface concentration and the thermodynamic evidence point to brush formation at $\Gamma > \Gamma^{**}$, the detailed structure of the brush cannot be inferred from the analysis of the ellipsometric data. Two different ellipsometric models for the interfacial film, (a) homogeneous swollen brush and (b) stratified brush (melt PPO film upon swollen PEO brush), give similar values of the ellipsometric angles in excellent agreement with the experimental data. The self-assembling scenario sketched in this work for PEO−PPO−PEO triblock copolymers at the air−water interface resembles the one previously described for end-capped PEO. The main difference is that in our case it is the more hydrophobic, but water-soluble, central PPO block that acts as the anchoring element at the interface, instead of the insoluble alkyl terminal segments.

The block size, characterized by the structural parameter β, plays an important role in the brush formation. From the comparative study for two different copolymers, it can be concluded that large central hydrophobic PPO blocks are able to accommodate in the air phase, and that the size of the anchoring head controls the grafting density, as expected.

Acknowledgment. This work was supported in part by the Fundación Ramón Areces and by DGES under Grant PB96-609. F.M. acknowledges the Centre d'Etudes de Physique Théorique et Nucléaire (CEPHYTEN, France) for financial support under contract 98/44-Institut Français du Pétrole. Dr. C. Mingotaud (CRPP) is also thanked for the realization of the BAM experiences and for helpful discussions. We thank the Centro de Espectroscopía (UCM, Spain) for the use of its facilities.

Appendix

To calculate the reflection coefficients, related to the ellipsometric angles Δ and Ψ through eq 2, from the constitutive parameters of the surface film (n = refraction index, d = thickness), an optical model for the interface must be proposed.

Model 1 or Single Homogeneous Film. Let us consider a single film made of melt polymer. If the thickness d is small enough in comparison with the wavelength of the incident light λ, if the film is optically isotropic ($n_x = n_y = n_z = n$), and if the thermally induced surface roughness is neglected, the Drude approximation for the change in the ellipsometric angle Δ caused by the single film can be used:[34]

$$\frac{\delta\Delta}{4\pi} = -\frac{d}{\gamma}\sin\theta tg\theta {n_1}^2 n_2 \frac{{n_1}^2 + {n_2}^2 - n^2 - ({n_1}^2{n_2}^2/n^2)}{({n_1}^2 - {n_2}^2)({n_1}^2 - {n_2}^2 tg^2\theta)} \quad \text{(A.1)}$$

where θ is the incidence angle.

On the other hand, Ψ does not change much with film thickness; it is mainly the refractive index of the subphase that causes Ψ to slightly increase with respect to the value for the free surface Ψ_0.

Model 2 or Swollen One-Layer Brush. The so-called microscopic model can be optically viewed as a one-layer composite film made of polymer chains dangling in the water subphase. Such a polymeric film, strongly swollen by the solvent, has an intermediate refractive index between those values for the pure polymer and water. By supposing the microscopic assembly pictured in Figure 7, one views the polymer brush as a rectangular package made of spherical elements of radius r where the fraction of interstitial volume ϕ_w, occupied by solvent molecules, represents the $100(1 - \pi/6) \approx 48\%$ of the total space $4r^2$. To estimate the refraction index, a volume average over the air, water, and polymer components will be used:[50]

$$\left(\frac{n^2 - 1}{n^2 + 2}\right) = \phi_p\left(\frac{{n_p}^2 - 1}{{n_p}^2 + 2}\right) + \phi_w\left(\frac{{n_w}^2 - 1}{{n_w}^2 + 2}\right) \quad \text{(A.2)}$$

The air contribution is zero ($n_a \approx 1$), and the total volume of the film is

$$\phi_q + \phi_w = 1 \quad \text{(A.3)}$$

From this approach, the averaged value of the refractive index of the brush may be calculated, and the film thickness d directly obtained from the experimental $\delta\Delta$ values via the Drude equation (see eq A.1).

Model 3 or Two-Layer Stratified Brush. To explain the ellipsometric data, more complex multilayered interfacial models could be postulated. Particularly, if stratification does exist within the film, multiple reflections and refractions in the optically different superposed films might be considered. In practice, a consecutive computation of Fresnel's coefficients for the involved interfaces, by taking the recalculated value of the incidence angle for each, is performed:[51]

$$R_p^{(ij)} = \frac{n_j\cos\theta_i - n_i\cos\theta_j}{n_j\cos\theta_i + n_i\cos\theta_j}$$

$$R_s^{(ij)} = \frac{n_i\cos\theta_i - n_j\cos\theta_j}{n_i\cos\theta_i + n_j\cos\theta_j} \quad \text{(A.4)}$$

where −s and −p read for both polarizations and i and j for both media defining each reflecting interface and θ is the incident angle, which is recalculated via Snell's law.

The ellipsometric angles are then computed as a function of thickness d by using the basic ellipsometric equation (eq 2).

Particularly, a two-layer model has been tentatively proposed to perform a detailed description of the brush. A swollen brush, made only of hydrophilic PEO blocks, with thickness d is supposed to be solubilized in water in contact with the aqueous subphase, while at the top, a thin film of melt PPO blocks lies adsorbed at the air−water interface.

LA990142A